Journal of Pharmaceutical and Biomedical Analysis 115 (2015) 431–442

Journal of Pharmaceutical and Biomedical Analysis

journal homepage: www.elsevier.com/locate/jpba

Analytical and statistical comparability of generic enoxaparins from the US market with the originator product

Pierre A.J. Mourier[a,*], Christophe Agut[b], Hajer Souaifi-Amara[c], Fréderic Herman[a], Christian Viskov[a]

[a] *Sanofi, 13, Quai Jules Guesde, 94403 Vitry-sur-Seine, France*
[b] *Sanofi R&D, 371, rue du Professeur Joseph, 34184 Montpellier, France*
[c] *External consultant from Experis™ IT, Life Sciences, 92723 Nanterre, France for CMC Biostatistics & Programming, Sanofi, Centre de recherche Vitry-sur-Seine, 13, quai Jules Guesde, 94403 Vitry-sur-Seine, France*

ARTICLE INFO

Article history:
Received 5 June 2015
Received in revised form 22 July 2015
Accepted 26 July 2015
Available online 29 July 2015

Keywords:
Analytical comparability
Disaccharide quantification
Enoxaparin
Generic
Chemometrics
Nuclear magnetic resonance

ABSTRACT

Low-molecular-weight heparins (LMWHs) are complex anticoagulant drugs, made from heparin porcine mucosa starting material. Enoxaparin sodium manufactured by Sanofi is one of the most widely prescribed LMWHs and has been used since 1993 in the USA. In 2010, US Food and Drug Administration approval for supplying generic enoxaparin was granted to Sandoz and subsequently to Amphastar. Little is known, however, of the differences in composition of these preparations. In this study, samples from several batches of generic enoxaparins were purchased on the US market and analyzed with state of the art methodologies, including disaccharide building blocks quantification, nuclear magnetic resonance (NMR), and a combination of orthogonal separation techniques. Direct high-performance liquid chromatography analysis of the different enoxaparin batches revealed distinct process fingerprints associated with each manufacturer. Disaccharide building block analysis showed differences in the degree of sulfation, the presence of glycoserine derivatives, as well as in proportions of disaccharides. Results were compared by statistical approaches using multivariate analysis with a partial least squares discriminant analysis methodology. The variations were statistically significant and allowed a clear distinction to be made between the enoxaparin batches according to their manufacturer. These results were further confirmed by orthogonal analytical techniques, including NMR, which revealed compositional differences of oligosaccharides both in low- and high-affinity antithrombin fractions of enoxaparin.

1. Introduction

Enoxaparin is a low-molecular-weight heparin (LMWH) widely used in clinical practice for the prevention and treatment of thromboembolism. Intestinal porcine heparin is used as a starting material in manufacturing LMWH. Heparin is biosynthesized in mast cells and certain other types of granulated cells as a proteoglycan. The heparin polysaccharide backbone consists of a heteropolymer comprised of alternating sugar units of 2-deoxy-2-sulfamido-α-D-glucopyranose (*N*-sulfated, or *N*-acetylated, *O*-sulfated) and *O*-sulfated uronic acids (α-L-iduronic acid or β-D-glucuronic acid). The arrangement of the disaccharide building blocks within the macromolecule is governed by both its biosynthesis and any microheterogeneity resulting from incomplete enzymatic reactions (such as deacetylation, *N*- and 2, 6-*O* sulfations). Some particular domains, the antithrombin III (ATIII) binding regions or alternatively pentasaccharide sequences, are 3-*O* sulfated and are mainly responsible for the anticoagulant activity

Abbreviations: AT, antithrombin; ATIII, antithrombin III; BSA, bovine serum albumin; CNBr, cyanogen bromide; CTA, cetyltrimethylammonium; CZE, capillary zone electrophoresis; EMA, European Medicines Agency; FDA, US Food and Drug Administration; Gal, galactose; GlcA, glucuronic acid; GPC, gel permeation chromatography; HILIC, hydrophilic interaction liquid chromatography; HPLC, high-performance liquid chromatography; HSQC, heteronuclear single quantum correlation spectroscopy; LMWH, low-molecular-weight heparin; mAU, milliabsorbance units; MS, mass spectrometry; NIPALS, non-linear iterative partial least squares; NMR, nuclear magnetic resonance; PLS-DA, partial least squares discriminant analysis; RSD, relative standard deviation; SAX, strong anion exchange; SD, standard deviation; Ser, serine; TPPI, time proportional phase incrementation; VIP, variable importance in the projection; Xyl, xylose.

* Corresponding author. Fax: +33 158 933908.
E-mail addresses: pierre.mourier@sanofi.com (P.A.J. Mourier), christophe.agut@sanofi.com (C. Agut), Hajer.souaifi-amara-ext@sanofi.com (H. Souaifi-Amara), frederic.herman@sanofi.com (F. Herman), christian.viskov@sanofi.com (C. Viskov).

http://dx.doi.org/10.1016/j.jpba.2015.07.038

Nomenclature

U	Uronic acid
IdoA	L-Iduronic acid: α-L–Idopyranosyluronic acid
GlcA	D-Glucuronic acid: β-D-glucopyranosyluronic acid
ΔU	4,5-Unsaturated uronic acid, e.g. ΔGlcA: 4-deoxy-α-L-threo-hex-enepyranosyluronic acid
GlcNAc	D-*N*-Acetyl glucosamine: 2-deoxy-2-acetamido-α-D-glucopyranose
GlcNS	D-*N*-Sulfate glucosamine: 2-deoxy-2-sulfamido-α-D-glucopyranose
2S	2-*O*-Sulfate
6S	6-*O*-Sulfate
3S	3-*O*-Sulfate
GalA	D-Galacturonic acid

Structural symbols

ΔIVa	ΔU-GlcNAc
ΔIVs	ΔU-GlcNS
ΔIIa	ΔU-GlcNAc,6S
ΔIIIa	ΔU 2S-GlcNAc
ΔIIs	ΔU-GlcNS,6S
ΔIIIs	ΔU 2S-GlcNS
ΔIa	ΔU 2S-GlcNAc,6S
ΔIs	ΔU 2S-GlcNS,6S
ΔIVs_{gal}	ΔGalA-GlcNS
ΔIIs_{gal}	ΔGalA-GlcNS,6S

The iduronic (id) or glucuronic (glu) structure of uronic acids is indicated for oligosaccharides, e.g. ΔIs IIIs$_{id}$. Underlined disaccharides have a 3-O-sulfated glucosamine

$\underline{\Delta IIs}$	ΔU-GlcNS,3S,6S
$\underline{\Delta Is}$	ΔU2S-GlcNS,3S,6S
$\underline{IIs_{glu}}$	GlcA-GlcNS,3S,6S
ΔIIa-$\underline{IIs_{glu}}$	ΔU-GlcNAc,6S- GlcA-GlcNS,3S,6S

of heparin by binding to antithrombin (AT) [1–3], a serine protease inhibitor of the serpin family. Heparin acts as a cofactor for AT by modifying its three-dimensional conformation, thus accelerating the inactivation of clotting factors, most importantly, that of Factor Xa and thrombin [3]. The initial step of the synthesis of enoxaparin is the partial esterification of the heparin polymer into a benzyl ester. This is followed by a depolymerization step using sodium hydroxide. The resulting mixture of polydisperse oligosaccharides increases the degree of complexity due to side reactions altering the endogenous disaccharide backbone during depolymerization [4]. Moreover, enoxaparin still contains ~20% of the total of the AT-binding fraction.

The most recent advances in analytical and separation methods have permitted the isolation and sequencing of a number of the active process-dependent components of enoxaparin [5]. It has also been demonstrated that the classic pentasaccharide sequences are located at different sites along the oligosaccharide chains [6]. However, despite such analytical advances, it remains impossible to make an exhaustive structural determination of all the components of an enoxaparin mixture. Indeed, the correct methodology for the production of generic enoxaparins has been a matter of extensive scientific debate [7,8].

Analytical guidelines have been proposed for the production of LMWH generics. The first generic enoxaparin was approved in 2010 for the US market. In parallel with agency recommendations (US Food and Drug Administration, FDA; European Medicines Agency, EMA) [8,9], a scientific advisory panel from the International Society on Thrombosis and Haemostasis also provided some related guidance [10]. As an example, they referred to the requirement for an identical compositional disaccharide analysis between the originator and the resulting biosimilar, taking into account the natural structural dispersion of unfractionated heparin. The recommendation was to use AT affinity chromatography as the best tool to discriminate high- and low-affinity fractions and to obtain an efficient mapping of the LMWH [10]. In spite of these recommendations, only one published work appears to have reported this method specifically for the analysis of LMWH [11].

High-performance liquid chromatography (HPLC) separations, with the exception of some cases, were usually unable to resolve mixtures above tetradecasaccharides [12], indicating that this technique alone is not satisfactory for comparability studies between enoxaparins. Although alternative methods were proposed, no single method can currently separate such a complex mixture. The key tests used for the quality assurance of LMWHs [13] are also not designed for such comparison since they lack sufficient resolution for separating their polysaccharide components. Zhang et al. proposed a combination of ultra-performance size exclusion chromatography/electrospray quadruple time-of-flight-mass spectrometry and capillary zone electrophoresis (CZE) for analyzing the components of LMWHs [14]. CZE was also used to analyze and quantify the building blocks of the various LMWHs, the most complex being enoxaparin, following their exhaustive depolymerization by heparinases. Although gel permeation chromatography (GPC)/mass spectrometry (MS) can indeed be useful to identify individual components, it is inappropriate to compare enoxaparin batches, as quantification by MS is difficult to achieve. It is also not possible to obtain a complete chromatogram of the mixture due to MS signal saturation. Li and coworkers proposed methods based on a combination of liquid chromatography and Fourier transform MS to analyze the composition of enoxaparin batches [15,16]. However, as previously highlighted, due to the absence of an AT affinity chromatography step, it was not possible to differentiate between the high-affinity oligosaccharides responsible for the anticoagulant activity and the remaining low-affinity material. Moreover, due to the low resolution of hydrophilic interaction liquid chromatography (HILIC), the oligosaccharide isomers of equivalent charge density (positional isomers generated by sulfates substitution pattern as well as the uronic acid configuration) are hardly separated [15].

A recent study assessed the identities of the originator and 330 generic enoxaparin batches available on the Brazilian market [17]. This structural investigation, based on a comparison analyzing the nuclear magnetic resonance (NMR) spectra of the originator compound on the GPC fractions, was, however, insufficient to characterize the structure of mixtures like enoxaparin. The basic determination of the 1,6-anhydro compounds [18] was also not performed. Furthermore, neither the chromatograms of enoxaparin nor its enoxaparin fractions were shown in this work. Thus the demonstration of the structural identity of different enoxaparin batches remains to be investigated.

It is our view that at least three chromatographic methods with orthogonal selectivity, such as affinity chromatography, GPC, and anion exchange, should be performed to allow, albeit with certain limitations, the assessment of the consistency between enoxaparins from different manufacturers. The purpose of this study was, therefore, to analyze and compare enoxaparin batches using 'state of the art' analytical methods. Additional simple methods, such as disaccharide compositional analysis as recommended in FDA guidelines [8], are also included. Enoxaparin batches from Sanofi (originator, 24 products), enoxaparin sodium injection Sandoz (hereinafter 'Sandoz', 9 products), and the US generic enoxaparin sodium injection Amphastar (hereinafter 'Amphastar', 4 products) were studied and compared. Inter-batch variability was assessed

and the products compared for each manufacturer. At the time of the study, the newly approved Teva enoxaparin generic was not available on the US market.

2. Materials and methods

2.1. Materials

Enoxaparin batches manufactured during the period 1999–2013 were studied as they are supplied in powder form. Other samples of generic enoxaparin purchased in the US were in syringes and were usually present at 100 mg/ml. All enzyme lyases from *Flavobacterium heparinum* (heparinase I [EC 4.2.7], heparinase II [no EC number], and heparinase III [EC 4.2.2.8]) were obtained from Grampian Enzymes (Aberdeen, UK). All other reagents and chemicals were of the highest quality available. Water was purified using a Millipore Milli-Q purification system (Darmstadt, Germany).

2.2. Exhaustive depolymerization by the heparinase mixture

Enoxaparin samples were digested into a mixture of disaccharides and tetrasaccharides using a mixture of enzyme lyases (heparinases) to quantify the building blocks of the examined sample as described previously for heparin samples [19].

2.2.1. Enzymatic digestion

The digestion of enoxaparin samples (20 μl of a 20 mg/ml solution in water) was performed at room temperature for 48 h in a total volume of 170 μl containing 20 μl of a mixture of heparinase I, II, and III, where each heparinase was at 0.5 IU/ml in a potassium phosphate buffer (pH 7.0; 10 mM KH_2PO_4 and 0.2 mg/ml of bovine serum albumin [BSA]) and 120 μl of sodium acetate buffer (pH 7.0; 100 mM) containing $Ca(OAc)_2$ (2 mM) and BSA (0.5 mg/ml) [19].

2.2.2. Analysis of heparin digests by strong anion exchange (SAX) chromatography

Digested samples of 4 μl to 10 μl were then injected on a column (250 × 3.2 mm) filled with Spherisorb SAX of 5 μm particle diameter (Waters, Guyancourt, France). The column temperature was set at 50 °C. Mobile phase A consisted of NaH_2PO_4 (pH 3.0; 1.8 mM), while mobile phase B was an aqueous solution of NaH_2PO_4 (1.8 mM) and 1 M $NaClO_4$ (pH 3.0; 1 M). A linear gradient (*t* 0 min%B 3; *t* 20 min%B 35; *t* 50 min%B 100) was applied to the column for the elution of the samples at a flow rate of 0.45 ml/min. Double UV detection was monitored at 232 nm and 202–247 nm. The *N*-acetylated oligosaccharide selective signal (202–247 nm) is the result of the subtraction of the 202 nm wavelength UV signal from the 247 nm reference signal, as previously described [20].

2.2.3. Principle of quantification

The quantification was based on the well-established assumption of the uniformity of the molar response coefficients at 232 nm (maximum of UV absorbance of unsaturated oligosaccharides obtained after heparinase digestion) [21,22]. The principle and the chromatographic method are identical to those used in the U.S. Pharmacopeia for the quantification of 1,6-anhydro derivatives in enoxaparin [18]. The percentage w/w for each component was given by the following formula:

$$\%\frac{w}{w} = \frac{100 \times Mw_1 \times A_i}{\Sigma_x Mw_x \times A_x}$$

where Mw_i and A_i represent the molecular weight and the chromatographic area at 232 nm of the assayed component *i*, respectively; Mw_x and A_x represent the molecular weight and the chromatographic area, respectively, of either the peak *X* or the zone *X* specified by its retention time. The sum is related to all the components eluted. The molecular weights of the peaks are given as described in Fig. 1, according to their identification on the chromatogram.

The precision of the method for LC evaluation of disaccharide building blocks was assessed in its application for the quantification of 1,6-anhydro derivatives in enoxaparin [18]. Repeatability experiments showed a relative standard deviation (RSD) of 1.3%, as based on the percentage of oligosaccharide chains in enoxaparin with 1,6-anhydro sequences (sum of three 1,6-anhydro building blocks [Fig. 2]).

The identification of chromatographic peaks has been already described in the case of heparin. The identity of the supplementary peaks eluted from the enoxaparin batches are illustrated in Fig. 2.

The initiation of heparin biosynthesis occurs at a specific sequence, glucuronic acid-galactose-galactose-xylose-serine (GlcA—Gal-Gal-Xyl-Ser), called glycoserine. The original glycoserine tetrasaccharide ΔGlcA β1-3 Gal β1-3 Gal β1-4 Xyl β1-0-Ser (ΔGlyser), obtained through cleavage by heparinase III [23], is found in heparinase digests of crude heparins. However, it was observed that the serine end could, as a result of the Maillard reaction, generate coloration in the resulting enoxaparin batches that could diminish their shelf-life. Oxidation steps were, therefore, inserted in the purification process of heparin to modify the glycoserines [24]. The two oxidized glycoserine tetrasaccharides $\Delta Glyser_{ox1}$ and $\Delta Glyser_{ox2}$ (for structures, see Table 1S in the Supplementary data-a1 file) were identified and were eluted on the first part of the chromatogram of the digest as shown in Fig. 1. To enable a suitable comparison of the glycoserine derivatives present in the different enoxaparin batches, the amounts of each of these derivatives were added to give a sum of glycoserines (Σ(Glycoserine)). The sulfate/carboxylate ratio was calculated by adding the sulfate/carboxylate ratio contributions of all building blocks, taking into account their respective abundance.

2.3. Chromatographic methods for direct analysis of enoxaparin batches

The orthogonal analytical methodology applied to enoxaparin batches is summarized in Fig. 3.

2.3.1. Affinity chromatography on immobilized antithrombin (AT)

An AT-sepharose column (30 cm × 7 cm) prepared by coupling 2 g human AT to cyanogen bromide (CNBr)-activated Sepharose 4B (Sigma, Saint-Quentin Fallavier, France) as described by Höök et al. [25] was used to separate high- and low-affinity fractions using two injections of 100 mg of the enoxaparin batch. All experimental data are provided in the Supplementary data-a1 file (Fig. 1S).

2.3.2. Gel permeation chromatography (GPC)

GPC was used to separate the LMWHs according to the size of their oligosaccharide constituents (ranging from tetrasaccharides, hexasaccharides, octasaccharides, up to tetradecasaccharides). A column (100 cm × 2.6 cm) filled with Bio Gel P-30 (Bio-Rad, Marnesla-Coquette, France) circulated with $NaClO_4$ (0.2 N) at a flow of 0.6 ml/min permitted the injection of 50–200 mg of the product diluted in the mobile phase. High- and low-affinity fractions obtained from the affinity chromatography step were injected on this column, and double UV detection at 202 nm and 232 nm and refractometry were performed. Examples of GPC chromatograms of high- and low-affinity enoxaparin are shown in Fig. 4. High- and low-affinity fractions from tetrasaccharides to tetradecasaccharides were then collected and desalted on Sephadex G-10 (GE Healthcare, Vélizy-Villacoublay, France). After lyophilization, frac-

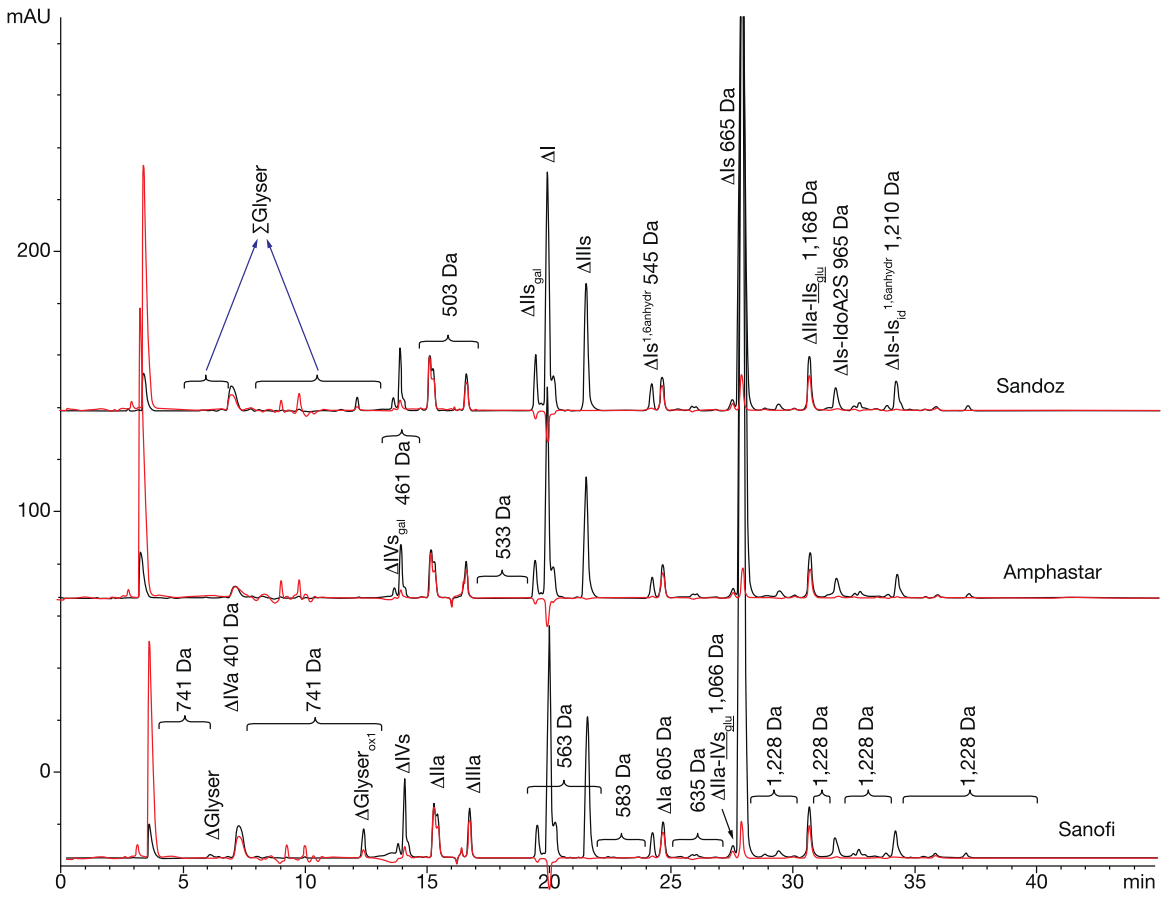

Fig. 1. Enoxaparin batches depolymerized by heparinase enzymes and separated by strong anion exchange chromatography (black lines: UV 234 nm; red lines: UV 202–242 nm). (For interpretation of the references to color in this figure legend, the reader is referred to the web version of this article.)

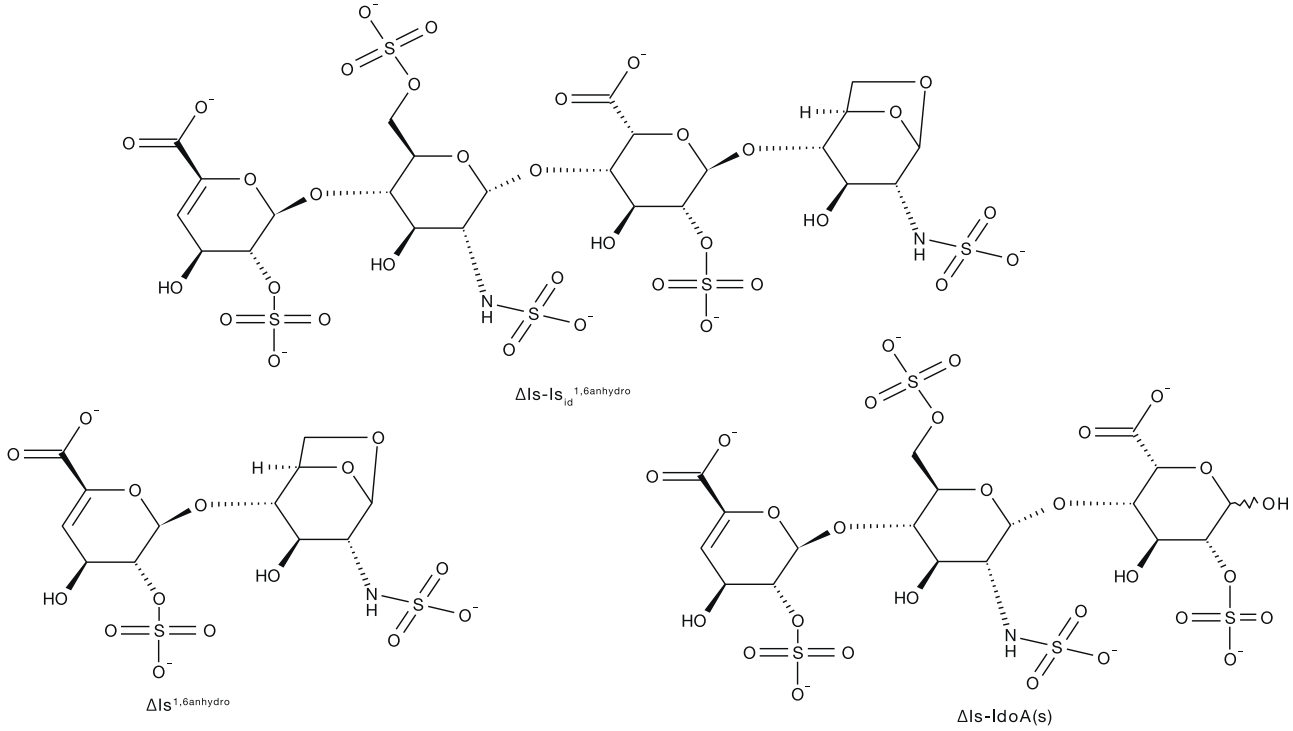

Fig. 2. Specific building blocks of enoxaparin present in the supplementary peaks eluted from enoxaparin.

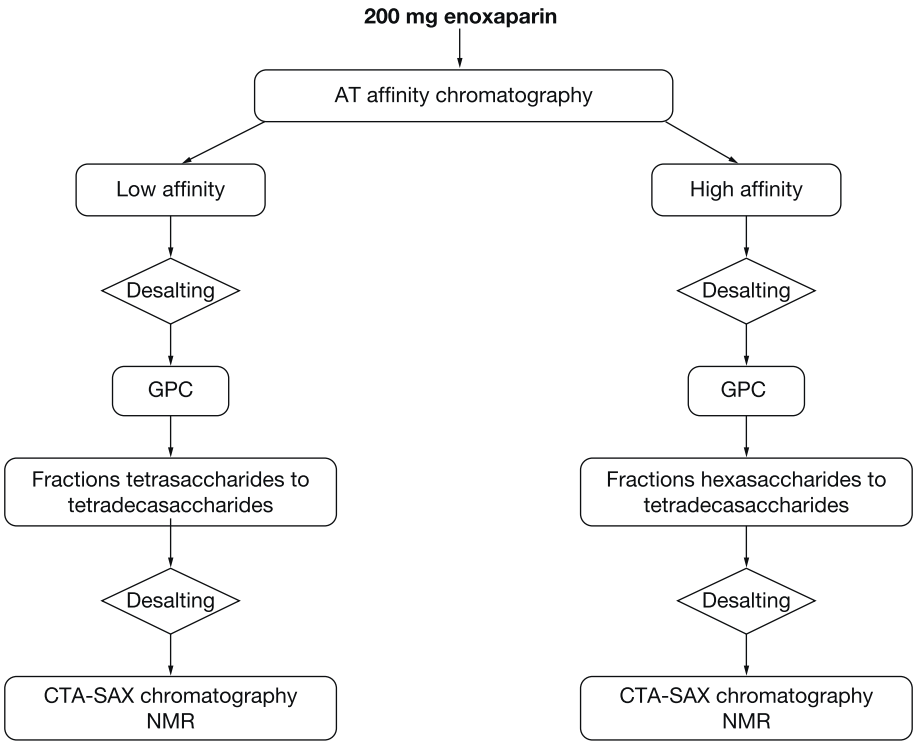

Fig. 3. Orthogonal analytical methodology used for the direct analysis of different sources of batches of enoxaparin. AT: antithrombin, CTA-SAX: cetyltrimethylammonium–strong anion exchange, GPC: gel permeation chromatography, NMR: nuclear magnetic resonance.

tions were ready for analysis either by cetyltrimethylammonium (CTA)-SAX HPLC or NMR.

2.3.3. Cetyltrimethylammonium (CTA)-SAX chromatography

CTA-SAX was used to analyze fractions purified by affinity chromatography and GPC. Columns filled with Kinetex C_{18} 2.6 μm particles (Phenomenex, Le Pecq, France) were prepared following a procedure described previously [20]. The mobile phases consisted of aqueous $NH_4CH_3SO_3$ (pH 2.5; concentrations varying between 0 and 2 M) and a flow rate of 0.22 ml/min. The column temperature was 40 °C and dual UV detection was performed at 232 nm and at 202–242 nm as described previously [20].

2.4. NMR

Enoxaparin tetradecasaccharide fractions were prepared by dissolving 2–5 mg of sample in 0.6 ml of D_2O 99.99% (Euriso-Top, Saint-Aubin, France). NMR spectra were recorded at 600 MHz on an Avance 600 spectrometer (Bruker BioSpin, Wissembourg, France) equipped with a 5 mm Triple Resonance (TXI) cryoprobe at a temperature of 25 °C, with pre-saturation of the residual water signals and with recycle delay of 3 s. 2D heteronuclear single quantum correlation spectra (HSQC) spectra were recorded with carbon decoupling during acquisition, using phase-sensitive echo/antiecho time proportional phase incrementation (TPPI) gradient selection (Bruker BioSpin standard sequence library). The polarization transfer delay was calculated with a $^1J_{C-H}$ coupling value of 150 Hz. Experiments were zero-filled and multiplied with sine-bell apodization prior to Fourier transformation.

2.5. Statistical analysis and data processing

The percentages weight/weight (% w/w) in the heparin chain of the 17 preselected building blocks were quantified for each of the 37 batches of enoxaparin tested (24 batches from Sanofi, and 13 from US generics: 9 from Sandoz and 4 from Amphastar). For confidentiality reasons, anonymous ID numbers were assigned to all batches (SAE1 to SAE24 for Sanofi batches, SZE1 to SZE9 for Sandoz batches, and AME1 to AME4 for Amphastar batches).

2.5.1. Exhaustive depolymerization by the heparinase mixture

From these data, average values, standard deviations (SDs), and SD/mean ratios were calculated for each building block.

2.5.2. Chemometrics and data analysis

A multivariate analysis utilizing a partial least squares discriminant analysis (PLS-DA) was used to compare the three producer groups of enoxaparin batches using the 17 preselected building blocks of the heparin chain. This popular technique in the field of chemometrics is especially suitable when the investigation concerns the prediction of a categorical variable from multi-collinear and non-normal predictors, which is common in chemical data analysis [26–29]. In the current study, it will be used to determine variables (from the 17 building blocks) enabling differentiation to be made between enoxaparins from different sources.

Prior to PLS-DA, all of the variables were centered and scaled to unit variance for comparison. The non-linear iterative partial least squares (NIPALS) algorithm was used to perform the PLS regression. The number of PLS components was selected by cross-validation.

After an initial PLS-DA analysis using all 17 variables, the most discriminating variables were selected from the variable importance in the projection (VIP) plot. Only those variables with VIP values higher than 1 were considered. These selected variables were then used to build a reduced PLS-DA model.

Discriminatory and predictive properties of models were assessed by the R^2 and Q^2 values provided by the software. The model validation was performed by cross-validation (based on 100 permutations).

In parallel, since the hypotheses of normality and homogeneity of variances were not fulfilled, a non-parametric univariate analysis

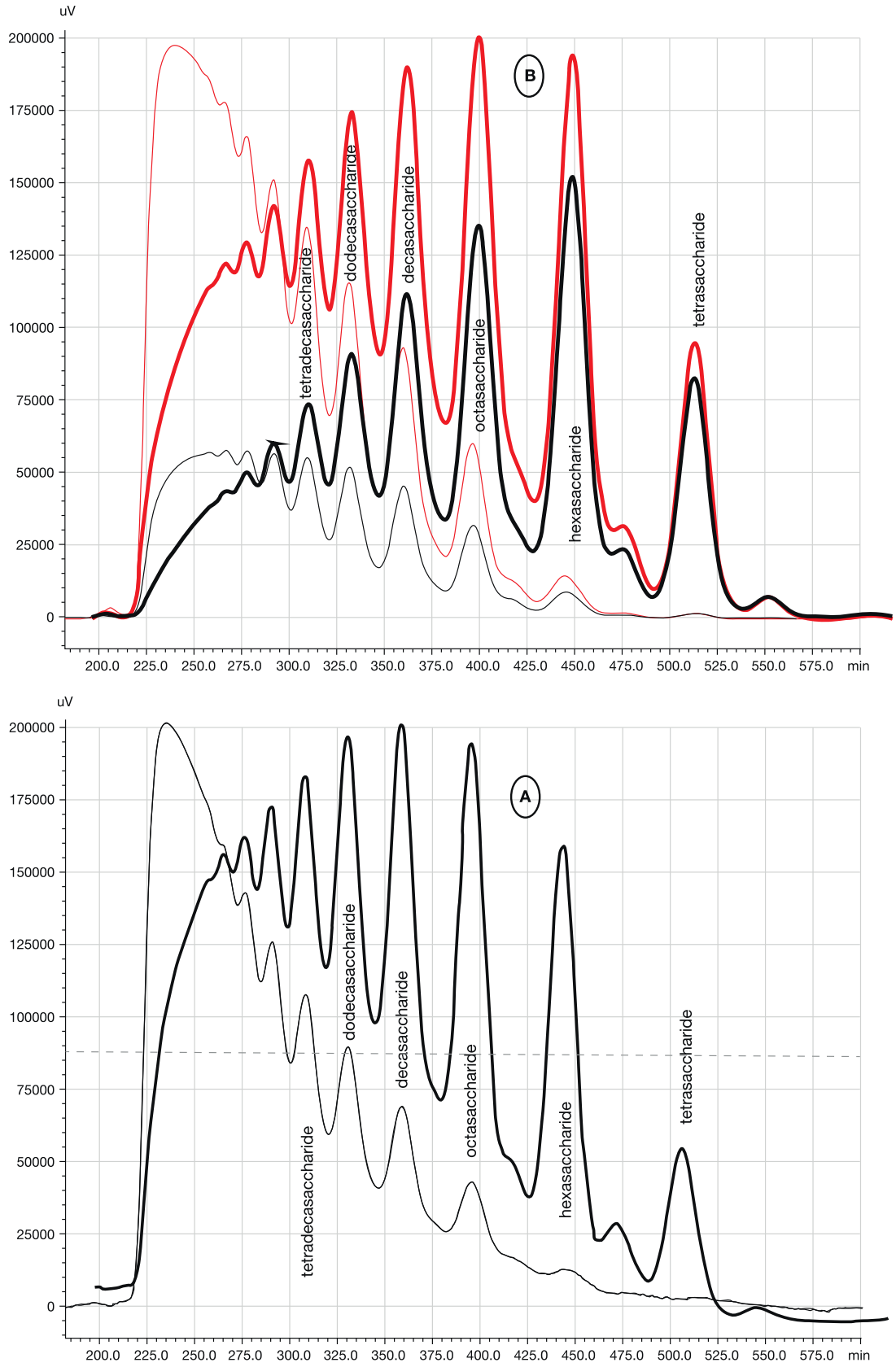

Fig. 4. Gel permeation chromatography (GPC) chromatograms of high-affinity (thin lines) and low-affinity (thick lines) enoxaparin. (A) Detection using a refractometer. (B) Detection using UV (black lines 232 nm; red lines: 202 nm). (For interpretation of the references to color in this figure legend, the reader is referred to the web version of this article.)

Table 1
Comparison of the average values, standard deviations (SD), and SD/average ratios obtained for the building blocks calculated from the originator Sanofi enoxaparin batches (Tables 2S and 3S in Supplementary data-a1 file), generic Sandoz enoxaparin batches (Table 4S in Supplementary data-a1 file), and generic Amphastar enoxaparin batches (Table 5S in Supplementary data-a1 file). Values are weight/weight (w/w) percentages of the building blocks obtained after exhaustive depolymerization of enoxaparin by heparinases.

	Sanofi			Sandoz			Amphastar		
Building blocks	Average	SD	% SD/ave	Average	SD	% SD/ave	Average	SD	% SD/ave
ΔIVa	1.7	0.2	12	1.3	0.2	18	0.7	0.2	29
Σ(Glyser)	1.5	0.4	26	1.3	0.3	19	0.3	0.0	14
ΔIVs_{gal}	0.2	0.1	30	0.2	0.1	35	0.2	0.1	29
ΔIVs	2.0	0.2	11	1.6	0.1	9	1.4	0.1	5
ΔIIa	2.6	0.3	10	2.7	0.3	10	2.3	0.1	4
ΔIIIa	1.2	0.1	7	1.0	0.1	7	1.1	0.1	14
ΔIIs_{gal}	1.0	0.4	44	1.5	0.3	17	1.8	0.3	14
ΔIIs	8.6	0.3	4	8.9	0.3	3	8.5	0.3	4
ΔIIIs	5.5	0.2	4	5.0	0.1	3	4.9	0.2	4
$\Delta Is^{1,6anhydr}$	1.1	0.2	16	1.1	0.2	20	0.7	0.0	6
ΔIa	1.3	0.3	19	1.4	0.1	7	1.4	0.0	2
$\Delta IIa\text{-}\underline{IVs_{glu}}$	0.9	0.1	9	0.8	0.1	8	0.8	0.3	32
ΔIs	58.9	0.7	1	59.2	1.0	2	62.3	0.9	1
$\Delta IIa\text{-}\underline{IIs_{glu}}$	4.2	0.2	4	4.6	0.2	5	4.3	0.3	6
ΔIs-IdoA2S	1.3	0.2	18	1.6	0.2	12	1.5	0.4	27
$\Delta Is\text{-}Is_{id}{}^{1,6anhydr}$	2.5	0.3	10	2.5	0.5	18	2.0	0.2	11
Sulf/Carb	2.4	0.0	1	2.4	0.0	1	2.5	0.0	1

Table 2
Wilcoxon pairwise comparison tests of the 5 most discriminant variables (variable importance in projection [VIP] > 1). *p*-values were corrected using the Bonferroni–Holm adjustment for multiple comparisons.

Comparison		ΔIVa	∑(Glyser)	ΔIVs	ΔIIIa	ΔIIIs
Sanofi	Sandoz	***p*** = 0.0051	*p* = 0.2221	***p*** = 0.0005	***p*** = 0.0001	***p*** < 0.0001
Sanofi	Amphastar	***p*** = 0.0051	***p*** = 0.0052	***p*** = 0.0033	*p* = 0.0860	***p*** = 0.0037
Sandoz	Amphastar	***p*** = 0.0184	***p*** = 0.0129	***p*** = 0.0316	*p* = 0.4808	*p* = 0.7530

Significant *p*-values at the 5% significance level are highlighted in bold. If $p < 0.05$, then the medians of parameter for the two compared groups are significantly different at the 5% significance level.

was chosen first to estimate the Spearman correlation coefficients. The differences in the median of the % w/w building blocks between the three groups of enoxaparin batches were then tested globally using the non-parametric Kruskal–Wallis test at a 5% significance level and, then post hoc, two by two, with Wilcoxon tests at a 5% significance level corrected for multiplicity by the Bonferroni–Holm adjustment.

2.5.3. Software

The PLS-DA was performed using SIMCA-PTM software (version 13.0.0.0 published by Umetrics AB, Umea, Sweden) [30], and univariate analysis was performed using SAS/STAT® software (version 9.2 of the SAS System for Windows, SAS Institute, Cary, NC) [31] and JMP® software (version 10.0.1) [32].

3. Results and discussion

3.1. Exhaustive depolymerization by the heparinase mixture

This study, based on determination of building blocks, was conducted after exhaustive depolymerization by heparinases on all the samples. Complete data analysis is provided in the Supplementary data-a1 file (Tables 2S to 5S). The average values, SDs, and SD/average ratio calculated for each building block of the 37 different enoxaparin batches are shown in Table 1.

As a general feature, the high SD/average ratios (>10%) were obtained with those building blocks, such as ΔIVs_{gal}, ΔIVs, ΔIIa, ΔIIIa, and ΔIa, which were present in small amounts. Higher deviation ratios were also obtained for the ΔIIs_{gal} and ΔIVs_{gal} disaccharides formed by alkaline 2-*O* desulfation. However, as this side reaction occurs during the preparation of both enoxaparin and heparin, its magnitude is dependent upon the heparin source used as starting material. This is not necessarily the same source between manufacturers. The case of the 1,6-anhydro building blocks is also notable. The depolymerization of $\Delta Is\text{-}Is_{id}{}^{1,6anhydr}$ into $\Delta Is^{1,6anhydr}$ by heparinase II is difficult and can possibly be incomplete. In that case, lower $\Delta Is^{1,6anhydr}$ values occur with higher levels of $\Delta Is\text{-}Is_{id}{}^{1,6anhydr}$. As a result, high SD/average ratios for $\Delta Is^{1,6anhydr}$ and $\Delta Is\text{-}Is_{id}{}^{1,6anhydr}$ only produce small differences in the depolymerization by heparinases of these particular building blocks. Enoxaparin batches from Amphastar showed lower averages for ΔIVa, ∑(Glyser) and higher averages for ΔIs when compared with enoxaparin batches from Sanofi and Sandoz.

3.2. Analysis of disaccharide building blocks quantification

The reduced PLS-DA model was built from 8 variables (ΔIIIs, ΔIIIa, $\Delta IIa\text{-}\underline{IIs_{glu}}$, ΔIs, Sulf/Carb, ∑(Glyser), ΔIVa, and ΔIVs) that had a VIP > 1 (Fig. 5A). Using the two PLS-DA components (c_1 and c_2), the cross-validated model was highly valid and predictive for each group of batches. In fact, for each group of batches, the intercept of Q^2_{cum} was negative (−0.238 for Sanofi batches, −0.208 for Sandoz batches, and −0.225 for Amphastar batches). The PLS-DA also demonstrated good discriminatory and predictive performances, with $R^2Y = 0.68$ ($R^2Y_{c1} = 0.42$ and $R^2Y_{c2} = 0.26$) and $Q^2Y = 0.63$.

Among the 17 building blocks, ΔIIIs, ΔIIIa, $\Delta IIa\text{-}\underline{IIs_{glu}}$, ΔIs, Sulf/Carb, ∑(Glyser), ΔIVa, and ΔIVs showed the highest discriminatory power, with a VIP higher than 1 (Fig. 5A). The ΔIVs_{gal}, ΔIa, and $\Delta IIa\text{-}\underline{IVs_{glu}}$ building blocks were the least discriminating variables from the VIP plot, with a VIP around 0.7 (< to the threshold of 1) (Fig. 5A). A Kruskal–Wallis test, at a 5% significance level, confirmed that the origin of the enoxaparin batches had no significant influence on these building blocks (p-value [ΔIVs_{gal}] = 0.2011, p-value [ΔIa] = 0.9473, p-value [$\Delta IIa\text{-}\underline{IVs_{glu}}$] = 0.1085).

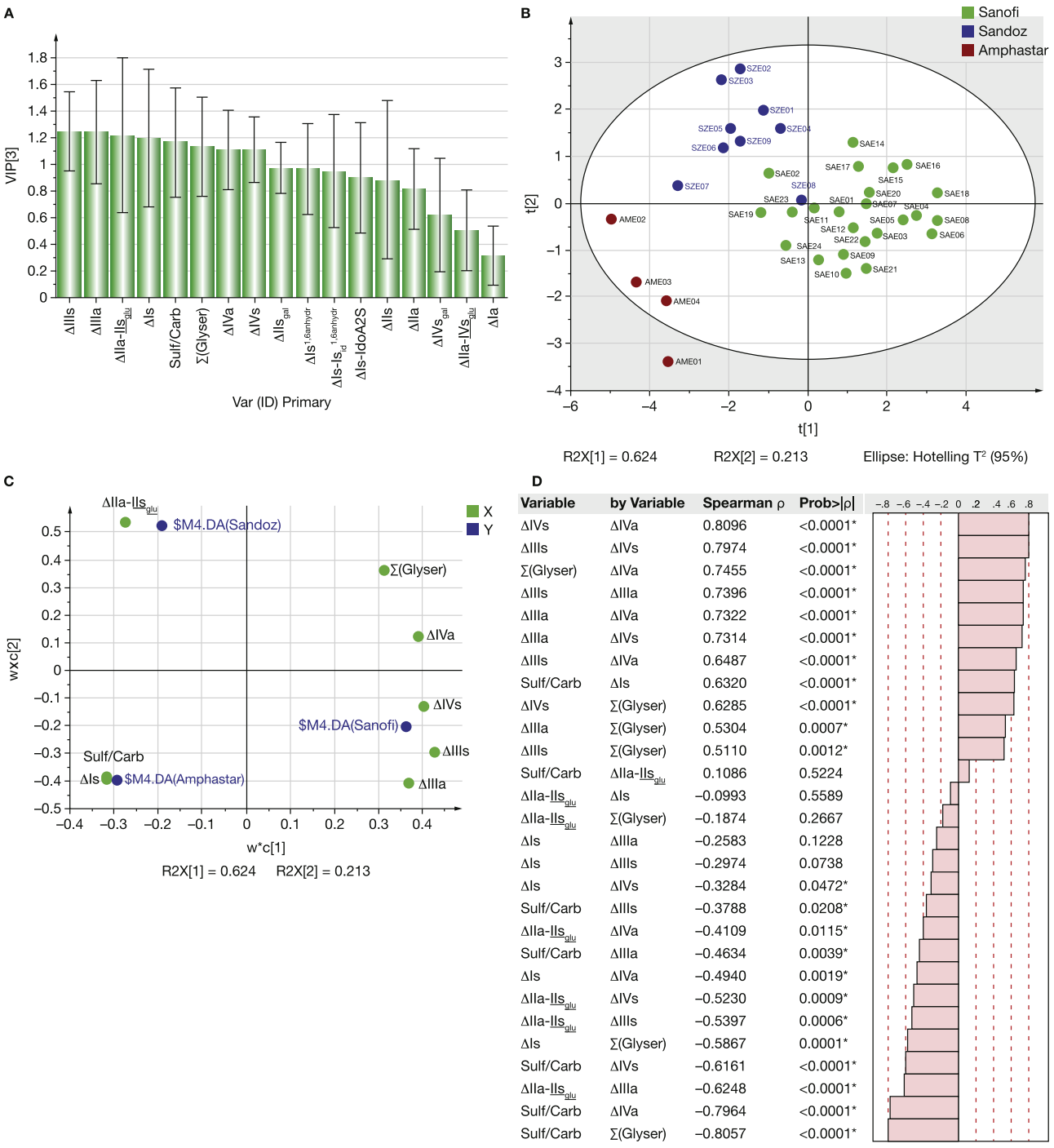

Variable	by Variable	Spearman ρ	Prob>|ρ|
ΔIVs	ΔIVa	0.8096	<0.0001*
ΔIIIs	ΔIVs	0.7974	<0.0001*
∑(Glyser)	ΔIVa	0.7455	<0.0001*
ΔIIIs	ΔIIIa	0.7396	<0.0001*
ΔIIIa	ΔIVa	0.7322	<0.0001*
ΔIIIa	ΔIVs	0.7314	<0.0001*
ΔIIIs	ΔIVa	0.6487	<0.0001*
Sulf/Carb	ΔIs	0.6320	<0.0001*
ΔIVs	∑(Glyser)	0.6285	<0.0001*
ΔIIIa	∑(Glyser)	0.5304	0.0007*
ΔIIIs	∑(Glyser)	0.5110	0.0012*
Sulf/Carb	ΔIIa-IIs glu	0.1086	0.5224
ΔIIa-IIs glu	ΔIs	−0.0993	0.5589
ΔIIa-IIs glu	∑(Glyser)	−0.1874	0.2667
ΔIs	ΔIIIa	−0.2583	0.1228
ΔIs	ΔIIIs	−0.2974	0.0738
ΔIs	ΔIVs	−0.3284	0.0472*
Sulf/Carb	ΔIIIs	−0.3788	0.0208*
ΔIIa-IIs glu	ΔIVa	−0.4109	0.0115*
Sulf/Carb	ΔIIIa	−0.4634	0.0039*
ΔIs	ΔIVa	−0.4940	0.0019*
ΔIIa-IIs glu	ΔIVs	−0.5230	0.0009*
ΔIIa-IIs glu	ΔIIIs	−0.5397	0.0006*
ΔIs	∑(Glyser)	−0.5867	0.0001*
Sulf/Carb	ΔIVs	−0.6161	<0.0001*
ΔIIa-IIs glu	ΔIIIa	−0.6248	<0.0001*
Sulf/Carb	ΔIVa	−0.7964	<0.0001*
Sulf/Carb	∑(Glyser)	−0.8057	<0.0001*

Fig. 5. (A) Variable importance in projection (VIP) plot of the initial partial least squares discriminant analysis (PLS-DA) model. (B) Score scatter plot (t_1/t_2) of the reduced PLS-DA model. Green circles or ID numbers SAE01 to SAE24 correspond to Sanofi enoxaparin batches; blue circles or ID numbers SZE01 to SZE09 correspond to Sandoz enoxaparin batches; red circles or ID numbers AME01 to AME04 correspond to Amphastar enoxaparin batches. (C) Loading scatter plot ($w \times c_1/w \times c_2$) of the reduced PLS-DA model: PLS weight plot corresponding to Fig. 5B . (D) Spearman correlation coefficients of the 8 most discriminant variables (VIP > 1). * Denotes significant correlations.

Fig. 5B shows the t_1/t_2 score of the reduced PLS-DA model and the corresponding weights ($w \times c_1/w \times c_2$) of the samples. The PLS-DA model clearly shows clustering between the samples from each of the three manufacturers. It may be noted that the group of Amphastar enoxaparin batches (red circles, ID numbers AME01 to AME04) has no overlap with the other groups of enoxaparin batches from Sandoz (blue circles, ID numbers SZE01 to SZE09) and Sanofi (green circles, ID numbers SAE01 to SAE24). Two PLS-DA components explain 68% of the Y-variance. These results show clear discrimination between the enoxaparin batches from all three manufacturers.

The loading scatter plot ($w \times c_1/w \times c_2$) of the reduced PLS-DA model shown in Fig. 5C enabled the determination of those variables that contribute strongly to the separation of the different batches. It also permitted any correlations existing between the variables and the group of enoxaparin batches to be identified.

Correlations between variables could also been interpreted from their Spearman correlation coefficients ρ and their significance at the 5% level (Fig. 5D). From this it can be seen that the ΔIIIs, ΔIVs,

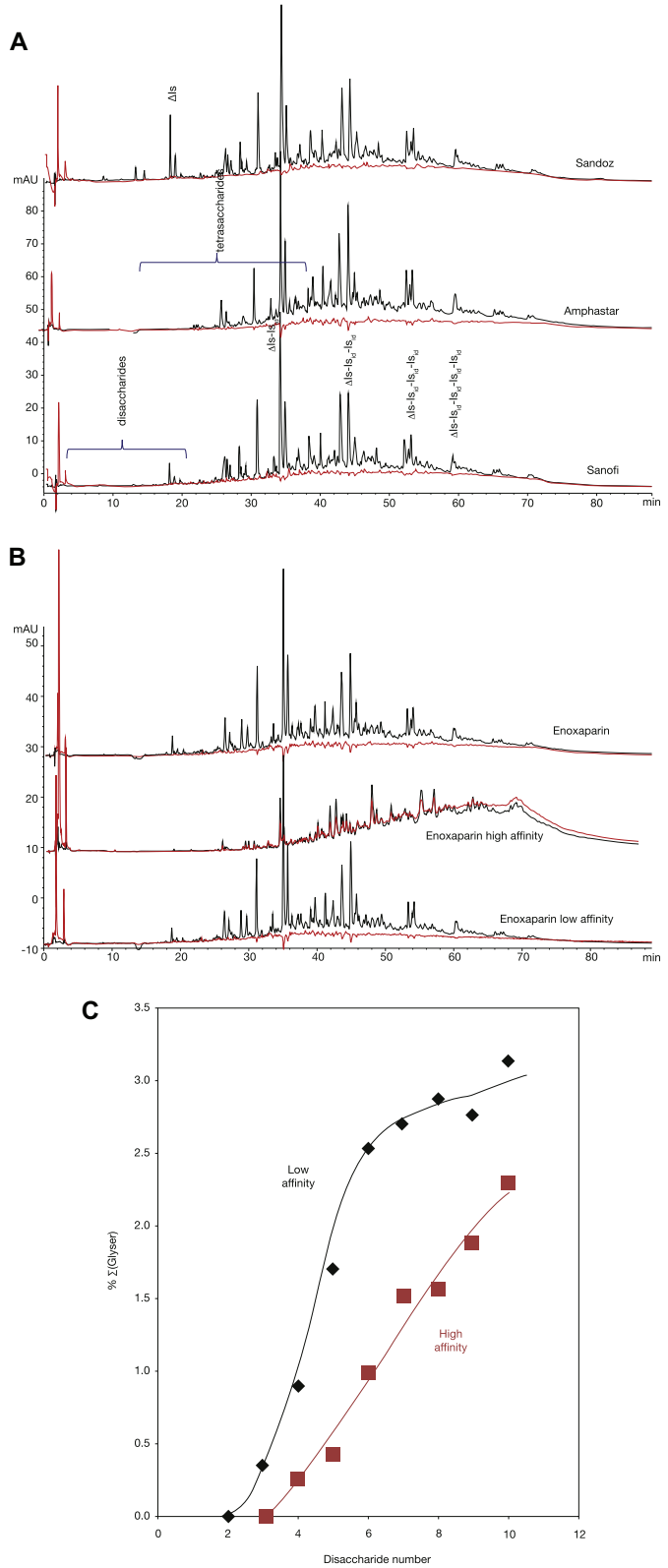

Fig. 6. (A) Cetyltrimethylammonium–strong anion exchange (CTA-SAX) chromatograms of originator Sanofi enoxaparin and generic Sandoz and Amphastar enoxaparin batches as they are (black line: UV 232 nm; red line: UV 202–242 nm). (B) CTA-SAX chromatograms of Sanofi enoxaparin as it is, and its high-affinity and low-affinity fractions (black lines: UV 232 nm; red lines: UV 202–242 nm). (C) Percentage of glycoserines (Σ(Glyser)) obtained after exhaustive depolymerization by heparinases of high- and low-affinity fractions as a function of the chain length (number of disaccharides). (For interpretation of the references to color in this figure legend, the reader is referred to the web version of this article.)

ΔIVa, ΔIIIa, and ∑(Glyser) were positively correlated ($r > 0.51$), as were the ΔIs and Sulf/Carb ($r = 0.63$). The ΔIIIs, ΔIIIa, and ΔIVs were negatively correlated to ΔIIa-$\overline{\text{IIs}_{glu}}$ ($r \geq 0.41$). ∑(Glyser) and ΔIVa were negatively correlated to ΔIs and Sulf/Carb ($r \geq 0.49$). ΔIs was not correlated to ΔIIIs (p-value = 0.0738), ΔIIIa (p-value = 0.1228), or ΔIIa-$\overline{\text{IIs}_{glu}}$ (p-value = 0.5589). ΔIIa-$\overline{\text{IIs}_{glu}}$ was not correlated to ΔIs (p-value = 0.5589), ∑(Glyser) (p-value = 0.2667), and Sulf/Carb (p-value = 0.5224).

Other variables discriminating between the different batches had significantly different medians according to the Wilcoxon pairwise comparison test as shown in Table 2. There were significant differences in the ΔIVs, ΔIIIs, ΔIIIa, ΔIVa, and ΔIIa-$\overline{\text{IIs}_{glu}}$ present in the Sanofi and Sandoz batches. Significant differences also occurred for ∑(Glyser), ΔIVa, ΔIVs, ΔIIIs, ΔIs, and Sulf/Carb in the comparison between the Sanofi and Amphastar batches, and for ∑(Glyser), ΔIVa, ΔIs, and Sulf/Carb present in the batches from Sandoz and Amphastar.

Results from the univariate and the multivariate analyses, therefore, allowed improved characterization of the composition of the disaccharide building blocks from the three different manufacturers of enoxaparin. In general, the Sandoz enoxaparin batches possessed significantly higher values of ΔIIa-$\overline{\text{IIs}_{glu}}$ but significantly lower values of ΔIIIa, ΔIIIs, ΔIVs, and ΔIVa than the Sanofi enoxaparin batches. Compared with Sanofi enoxaparin, significantly higher values of Sulf/Carb and ΔIs and significantly lower values of ∑(Glyser), ΔIVa, ΔIVs, ΔIIIs, and ΔIIIa were identified in the Amphastar enoxaparin batches. Compared to Sanofi enoxaparin, approximately 3% of the building blocks, i.e. low sulfated disaccharides concentrated on the reducing ends of the oligosaccharide chains, are missing in the Amphastar batches. The higher degree of sulfation of the Amphastar oligosaccharide chains (% ΔIs and Sulf/Carb ratio) could, at least partly, be the consequence of the missing low sulfated sequences.

3.3. CTA-SAX chromatograms of enoxaparin fractions

The CTA-SAX chromatographic analyses of the Sanofi and the generic Sandoz and Amphastar enoxaparin batches are shown in Fig. 6A. The whole oligosaccharide mixture present in the product and its diverse chain lengths can be shown in this type of chromatogram. These oligosaccharides possessed, however, an unsaturated uronic acid on their non-reducing end, giving a molar signal by UV detection at 232 nm. This resulted in emphasis on the presence of shorter oligosaccharidic chains (disaccharides to hexasaccharides representing only about 15% of the batches and 2–3% of the active ingredients) in the samples.

The disaccharides were eluted at retention times of less than 20 min, with obvious differences being observed for the three different sources of enoxaparin. These differences could be dependent on the last steps of purification of enoxaparin and, more specifically, on the respective workup conditions of the depolymerization process. These differences in composition between manufacturers were also visible for the tetrasaccharides. While these results are informative for the overall enoxaparin complex mixture, the inability to resolve larger components than hexasaccharides means that there is a strong overlap between the constituent molecules. In order to obtain a more precise view on the higher oligosaccharides composition, the use of additional orthogonal methods, such as those described in the scheme shown in Fig. 3, are essential. This point is emphasized in the present study by comparing eluted AT fractions. Fig. 6B shows a comparison of the high- and low-affinity AT fractions and the originator Sanofi enoxaparin. Despite the high-affinity fraction constituting 20–25% w/w of the batch, its higher molecular weight means that it can barely be detected in the chromatogram of the generic enoxaparin batch. Consequently,

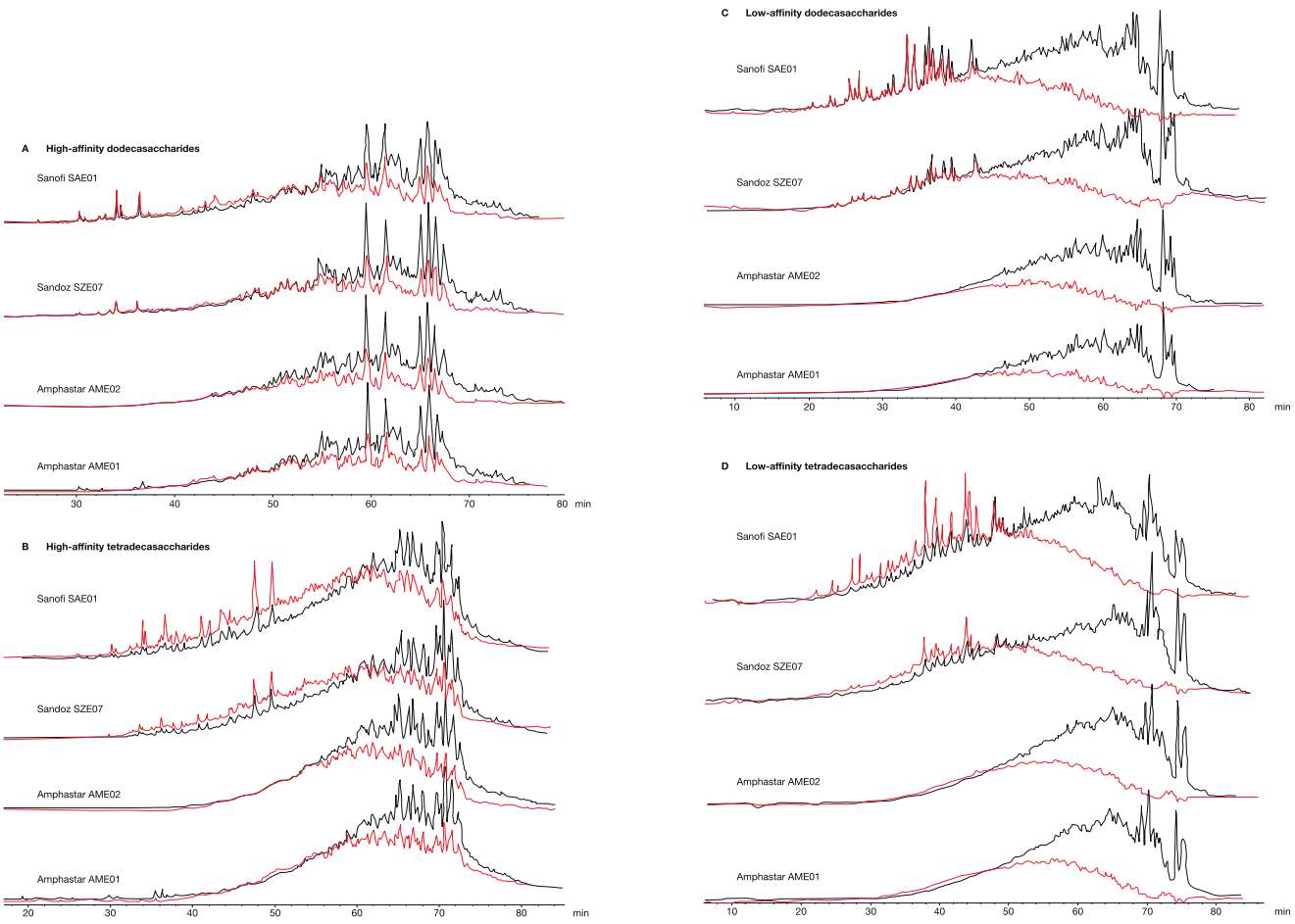

Fig. 7. Cetyltrimethylammonium–strong anion exchange (CTA-SAX) chromatograms of the Sanofi, Sandoz, and Amphastar enoxaparins (black lines: UV 232 nm; red lines: UV 202–242 nm). (A) High-affinity dodecasaccharides. (B) High-affinity tetradecasaccharides. (C) Low-affinity dodecasaccharides. (D) Low-affinity tetradecasaccharides. (For interpretation of the references to color in this figure legend, the reader is referred to the web version of this article.)

the chromatogram of the low-affinity fraction appears rather similar to that of the originator enoxaparin source, thus reinforcing the importance of using orthogonal methods to assess precisely the compositional aspects and to overcome overlapping broad peaks.

The subsequent use of CTA-SAX chromatography on the low-affinity samples and the AT affine fractionated according to the size of their components, i.e. disaccharides, tetrasaccharides, hexasaccharides, up to tetradecasaccharides, by GPC resulted in the generation of an important amount of data. The most relevant results are shown here, while the remainder are provided as Supplementary data-a1 and a2 files (Figs. 2S–10S). The data presented in this paper are focused primarily on the glycoserine-containing fractions. The percentage of oligosaccharide chains containing a glycoserine moiety at the reducing end increases with increasing chain length (Fig. 6C) and, as a result, these fractions mainly correspond to those chains longer than dodecasaccharides.

High-affinity dodecasaccharides and tetradecasaccharides from enoxaparin from the three manufacturers are compared in Figs. 7A and 7B. A similar comparison of the low-affinity fractions is shown in Figs. 7C and 7D. The glycoserine-containing oligosaccharides can easily be identified. The low sulfation of the reducing end saccharides induces a low retention time on the chromatogram (tr < 45 min for dodecasaccharides and tr < 50 min for tetradecasaccharides). These compounds are also highly acetylated and, consequently, strongly absorb at the UV selective signal of 202–242 nm.

Of all the fractions studied, only the Amphastar generic enoxaparin contained the higher sulfated components. Low sulfated oligosaccharides, i.e. the less retained compounds on the chromatograms, were not detected. The reason for this absence remains unclear but is probably dependent upon the manufacturing process. This observation also correlated with the results obtained after the exhaustive depolymerization by heparinases, indicating the presence of significantly lower amounts of glycoserine markers in the Amphastar batches.

3.4. NMR analysis of enoxaparin fractions

In view of the differences described above, the Sanofi and Amphastar enoxaparins were further compared by NMR spectroscopy using two-dimensional ^{1}H-^{13}C HSQC spectra. These results are all supplied in the Supplementary data-b file (Figs. 11S to 19S). Amphastar enoxaparin batches, as well as their low- and high-affinity fractions, exhibited spectra where the characteristic signal of glycoserine moieties was very weak and significantly less important than in those present in the Sanofi batches. Since glycoserines are mainly present in the high-molecular-weight fractions (Fig. 6C), the low- and high-affinity fractions above dodecasaccharides obtained from Amphastar and Sanofi showed different spectra due to the lack of glycoserine-containing oligosaccharides in Amphastar batches. These observations confirmed the data obtained from both the heparinase exhaustive depolymerization step as well as that from the CTA-SAX chromatograms. In the Amphastar enoxaparin batches, the very low presence of glycoserine ends and neighboring disaccharides (ΔIVa and ΔIVS) demonstrated the loss of

approximately 4–6 low sulfated saccharide units, thus increasing the sulfate/carboxylate ratio significantly.

4. Conclusions

We have defined a protocol for the analysis of originator and generic batches of enoxaparin. This study summarizes our analytical findings on representative batches of originator (Sanofi) and generic (Sandoz and Amphastar) enoxaparin. 'State of the art' methods, such as disaccharide building blocks analysis and direct CTA-SAX chromatography, were able to differentiate the enoxaparins supplied from three different manufacturers. Qualitative analysis of the CTA-SAX chromatogram (Fig. 6A) was helpful to observe differences in the enoxaparin manufacturing process workup and highlight characteristic fingerprint differences in their di- and tetrasaccharide compositions. Thus, the qualitative analysis of disaccharide building blocks described here shows that Amphastar enoxaparin has, for example, a significantly higher degree of sulfation and a lower glycoserine derivative content than both the Sanofi and Sandoz enoxaparins. These differences can be also observed in the compositional analysis of the polysaccharide mixtures (without enzymatic pretreatment) by using a combination of orthogonal methods, including NMR. They appear both in the AT affine oligosaccharide and non-affine fractions of enoxaparin products. The differences between the Sanofi and Sandoz enoxaparins are less intuitive, but are clearly revealed by the PLS-DA statistical analysis of their building blocks, which also show significant discrimination between the enoxaparins sourced from all three manufacturers. The clinical significance of these structural differences continues to be evaluated.

Conflict of interest

P. Mourier, C. Agut, F. Herman, and C. Viskov are employees of Sanofi. H. Souaifi-Amara is a Sanofi external consultant from Experis™ IT, Life Sciences, Nanterre, France.

Role of the funding source

The study was carried out by Sanofi R&D employees as part of their research duties. The external consultant was contracted by Sanofi for the work performed on this project. All authors contributed to the drafting of the manuscript with editorial assistance provided by a medical writer, paid for by Sanofi. The decision to submit the article for publication was shared by all authors.

Acknowledgments

This study was funded by Sanofi. Editorial support in the preparation of this article was provided by M. Calle, Excerpta Medica, funded by Sanofi.

Appendix A. Supplementary data

Supplementary data associated with this article can be found, in the online version, at http://dx.doi.org/10.1016/j.jpba.2015.07.038.

References

[1] M. Petitou, B. Casu, U. Lindahl, 1976–1983, a critical period in the history of heparin: the discovery of the antithrombin binding site, Biochimie 85 (2003) 83–89, http://dx.doi.org/10.1016/S0300-9084(03)78-6.
[2] M. Hricovini, A. Guerrini, G. Bisio, M. Torri, B. Petitou, Conformation of heparin pentasaccharide bound to antithrombin III, Biochem. J. 359 (2001) 265–272, PMID:11583572.
[3] A. Danielsson, E. Raub, U. Lindahl, I. Björk, Role of ternary complexes, in which heparin binds both antithrombin and proteinase, in the acceleration of the reactions between antithrombin and thrombin or factor Xa, J. Biol. Chem. 261 (1986) 15467–15473, PMID: 3782075.
[4] M. Guerrini, S. Elli, D. Gaudesi, G. Torri, B. Casu, P. Mourier, F. Herman, C. Boudier, M. Lorenz, C. Viskov, Effects on molecular conformation and anticoagulant activities of 1,6-anhydrosugars at the reducing terminal of antithrombin-binding octasaccharides isolated from low-molecular-weight heparin enoxaparin, J. Med. Chem. 53 (2010) 8030–8040, http://dx.doi.org/10.1021/jm100771s.
[5] C. Viskov, M. Just, V. Laux, P. Mourier, M. Lorenz, Description of the chemical and pharmacological characteristics of a new hemisynthetic ultra-low-molecular-weight heparin, AVE5026, J. Thromb. Haemost. 7 (2009) 1143–1151, http://dx.doi.org/10.1111/j.1538-7836.2009.03447.x.
[6] M. Guerrini, S. Guglieri, B. Casu, G. Torri, P. Mourier, C. Boudier, C. Viskov, Antithrombin-binding octasaccharides and role of extensions of the active pentasaccharide sequence in the specificity and strength of interaction. Evidence for very high affinity induced by an unusual glucuronic acid residue, J. Biol. Chem. 283 (2008) 26662–26675, http://dx.doi.org/10.1074/jbc.M801102200.
[7] P. Minghetti, F. Cilurzo, S. Franzé, U.M. Musazzi, M. Itri, Low molecular weight heparins copies: are they considered to be generics or biosimilars? Discov. Today 18 (2013) 305–311, http://dx.doi.org/10.1016/j.drudis.2012.11.002.
[8] FDA, Response to Citizen Petition Docket No. FDA-2003-P-0273A 2003. http://www.fda.gov/downloads/drugs/./guidances/ucm277709.pdf (accessed 13.05.15).
[9] European Medicines Agency, Concept paper on the revision of the guideline on non-clinical and clinical development of similar biological medicinal products containing low-molecular-weight heparins (EMA/CHMP/BMWP/522386/2011). The proposed guideline will replace Guideline on Non-clinical and Clinical Development of Similar Biological Medicinal Products Containing Low-Molecular-Weight Heparins, EMEA/CHMP/BMWP/118264/2007, European Medicines Agency, 2011.www.ema.europa.eu/docs/en_GB/document_library/Scientific_guideline/2011/07/WC500109588.pdf (accessed 13.05.15).
[10] J. Harenberg, J. Walenga, G. Torri, O.E. Dahl, L. Drouet, J. Fareed, Subcommittee on Control of Anticoagulation, Scientific and Standardization Committee of the International Society on Thrombosis and Haemostasis Update of the recommendations on biosimilar low-molecular-weight heparins from the Scientific Subcommittee on Control of Anticoagulation of the International Society on Thrombosis and Haemostasis, J. Thromb. Haemost. 11 (2013) 1421–1425, http://dx.doi.org/10.1111/jth.12269.
[11] A. Bisio, D. Vecchietti, L. Citterio, M. Guerrini, R. Raman, S. Bertini, G. Eisele, A. Naggi, R. Sasisekharan, G. Torri, Structural features of low-molecular-weight heparins affecting their affinity to antithrombin, Thromb. Haemost. 102 (2009) 865–873, http://dx.doi.org/10.1160/TH09-02-0081.
[12] P.A. Mourier, O.Y. Guichard, F. Herman, C. Viskov, Isolation of a pure octadecasaccharide with antithrombin activity from an ultra-low-molecular-weight heparin, Anal. Biochem. 453 (2014) 7–15, http://dx.doi.org/10.1016/j.ab.2014.02.013.
[13] H. Ye, T.K. Toby, C.D. Sommers, H. Ghasriani, M.L. Trehy, W. Ye, R.E. Kolinski, L.F. Buhse, A. Al-Hakim, D.A. Keire, Characterization of currently marketed heparin products: key tests for LMWH quality assurance, J. Pharm. Biomed. Anal. 85 (2013) 99–107, http://dx.doi.org/10.1016/j.jpba.2013.06.033.
[14] Q. Zhang, X. Chen, Z. Zhu, X. Zhan, Y. Wu, L. Song, J. Kang, Structural analysis of low molecular weight heparin by ultraperformance size exclusion chromatography/time of flight mass spectrometry and capillary zone electrophoresis, Anal. Chem. 85 (2013) 1819–1827, http://dx.doi.org/10.1021/ac303185w.
[15] L. Li, F. Zhang, J. Zaia, R.J. Linhardt, Top–down approach for the direct characterization of low molecular weight heparins using LC–FT–MS, Anal. Chem. 84 (2012) 8822–8829, http://dx.doi.org/10.1021/ac302232c.
[16] G. Li, J. Steppich, Z. Wang, Y. Sun, C. Xue, R.J. Linhardt, L. Li, Bottom–up low molecular weight heparin analysis using liquid chromatography-Fourier transform mass spectrometry for extensive characterization, Anal. Chem. 86 (2014) 6626–6632, http://dx.doi.org/10.1021/ac501301v.
[17] S.N. Oliveira, G.R. Santos, B.F. Glauser, N.V. Capillé, I.N. Queiroz, M.S. Pereira, V.H. Pomin, P.A. Mourão, Structural and functional analyses of biosimilar enoxaparins available in Brazil, Thromb. Haemost. 113 (2015) 53–65, http://dx.doi.org/10.1160/TH14-05-0411.
[18] U.S. Pharmacopeia–National Formulary (USP–NF), Test for 1,6-anhydro derivative for enoxaparin sodium, U.S. Pharmacopeial Convention, 2009. http://www.usp.org/sites/default/files/usp_pdf/EN/USPNF/genChapter207.pdf (accessed 13.05.15).
[19] P. Mourier, P. Anger, C. Martinez, F. Herman, C. Viskov, Quantitative compositional analysis of heparin using exhaustive heparinase digestion and strong anion exchange chromatography, Anal. Chem. Res. 3 (2015) 46–53, http://dx.doi.org/10.1016/j.ancr.2014.12.001.
[20] P.A. Mourier, C. Viskov, Chromatographic analysis and sequencing approach of heparin oligosaccharides using cetyltrimethylammonium dynamically coated stationary phases, Anal. Biochem. 332 (2004) 299–313, http://dx.doi.org/10.1016/j.ab.2004.06.020.
[21] K.G. Rice, R.J. Linhardt, Study of structurally defined oligosaccharide substrates of heparin and heparan monosulfate lyases, Carbohydr. Res. 190 (1989) 219–233, http://dx.doi.org/10.1016/0008-6215(89)84127-8.
[22] A. Pervin, C. Gallo, K.A. Jandik, X.J. Han, R.J. Linhardt, Preparation and structural characterization of large heparin-derived oligosaccharides, Glycobiology 5 (1995) 83–95, http://dx.doi.org/10.1093/glycob/5.1.83.

[23] S. Sugahara, K. Yamada, J.F. de Waard, A novel sulfated structure in the carbohydrate-protein linkage region isolated from porcine intestinal heparin, J. Biol. Chem. 267 (1992) 1528–1533, PMID: 1730699.
[24] C. Viskov, P. Mourier, Process for oxidizing unfractionated heparins and detecting presence or absence of glycoserine in heparin and heparin products, US patent (2005) https://www.lens.org/lens/patent/US_2005_0215519_A1/
[25] M. Höök, I. Björk, J. Hopwood, U. Lindahl, Anticoagulant activity of heparin: separation of high-activity and low-activity heparin species by affinity chromatography on immobilized antithrombin, FEBS Lett. 66 (1976) 90–93, http://dx.doi.org/10.1016/0014-5793(76)80592-3.
[26] I.E. Frank, J.H. Friedman, A statistical view of some chemometrics regression tools, Technometrics 35 (1993) 109–135, http://dx.doi.org/10.1080/00401706.1993.10485033.
[27] S. Wold, M. Sjöström, L. Eriksson, PLS-regression: a basic tool of chemometrics, Chemometr. Intell. Lab. Syst. 58 (2001) 109–130, http://dx.doi.org/10.1016/S0169-7439(01)155-1.
[28] M. Barker, W. Rayens, Partial least squares for discrimination, J Chemometr 17 (2003) 166–173. http://dx.doi.org/10.1002/cem.785
[29] R. Hastie, J. Tibshirani, J. Friedman, The Elements of Statistical Learning: Data Mining, in: Inference and Prediction, Springer, New York, 2009, http://dx.doi.org/10.1007/978-0-387-84858-7.
[30] Umetrics, SIMCA-online (version 13.0.0.0), http://www.umetrics.com/products/simca-online.
[31] SAS Institute Inc., SAS/STAT® 9.2, SAS Institute Inc., Cary, NC, 2010.
[32] SAS Institute Inc., JMP-online (version 10.0.1), http://www.jmp.com